

## **Biased electrodes for SOL control in NSTX**

**S.J. Zweben\***, R.J. Maqueda<sup>a</sup>, L. Roquemore, C.E. Bush<sup>b</sup>, R. Kaita,  
R.J. Marsala, Y. Raitses, R.H. Cohen<sup>c</sup>, D.D. Ryutov<sup>c</sup>

*Princeton Plasma Physics Laboratory, Princeton NJ USA*

*(a) Nova Photonics, Princeton NJ USA*

*(b) Oak Ridge National Laboratory, Oak Ridge TN USA*

*(c) Lawrence Livermore National Laboratory, Livermore, CA USA*

Small electrodes were installed in the outer-midplane edge of NSTX to attempt to control the local width of the scrape-off layer (SOL) by creating a outward  $E_{\text{pol}} \times B$  flow. When the applied voltage between electrodes was  $\pm 90$  volts, the density between these electrodes increased by a factor of 3-10 over a radial width of  $\sim 4$  cm. Thus a local control of the far-SOL plasma density was obtained.

## 1. Motivation and Previous Experiments

The present experiment was motivated by the theory that the scrape-off layer (SOL) width in a tokamak could be controlled by toroidally non-axisymmetric electrical biasing of divertor plates [1-3]. Such biasing would create a local poloidal electric field with a radial  $E_{\text{pol}} \times B$  drift larger than the normal radial flow velocity, and so radially move the local SOL strike position at the divertor plate. Similar ideas have also been proposed for RF-sheath generated convective cells near the outer midplane [4].

These ideas have been tested in several previous experiments. In JFT-2M [5] an electrical bias of +120 volts was applied to an inner wall divertor plate and a poloidal electric field of  $\sim 1$  kV/m was measured at the midplane where the magnetic field lines connected to the biased plate. In MAST [6] an electrical bias of +80 to +120 volts was applied to 6 toroidally separated divertor ‘ribs’, and a movement of the  $D_{\alpha}$  emission was seen at these ribs in the expected  $E \times B$  drift direction. In CASTOR [7] an electrode was biased +100 to +200 volts in the SOL, a poloidal electric field of up to 5 kV/m was created on flux surfaces connected to the electrode, and a strong poloidal modulation of the radial particle flux was

measured. In related experiments, a positive DC plate bias in DITE changed the floating potential in a probe  $\sim 2.5$  mm away along B [8], a positive DC and 30 kHz bias in TEXT were detected  $\sim 12$  m away along B [9], and a 60 KHz probe bias in W7-AS was observed at a distance up to  $\sim 12$  m away along B [10]. Thus several previous biasing experiments have created local poloidal electric fields in the SOL.

## **2. NSTX electrodes, probes, and biasing conditions**

The electrode configuration used for this experiment is shown in Fig. 1. Four 3 cm x 3 cm stainless steel electrodes were flush-mounted in a boron nitride holder with a poloidal gap of  $\sim 1$  cm between them. Each electrode could be independently biased up to  $\pm 100$  volts with respect to the local vessel wall and could draw up to 30 amps per electrode for positive bias, and 10 amps per electrode for negative bias. The electrode power supplies were modulated at 50 Hz for clearer comparison of electrode on and off states. This electrode holder was mounted  $\sim 20^\circ$  below the outer midplane and oriented so that the electrodes were spaced along the local poloidal direction and the total magnetic field was normal to the plane of the electrodes. The innermost radial edge of the electrode holder (which was not movable) was  $\sim 1$  cm behind the leading edge of an RF antenna limiter located just behind the electrode holder. Thus the electrodes were in

contact with the SOL plasma in only one direction along B, and the field lines in this direction extended  $\sim 1$  to  $\sim 8$  meters along B before hitting any other object in the SOL (depending on the details of the plasma equilibrium). The effect of the biasing was measured locally with a set of flush-mounted stainless steel Langmuir probes of diameter 3 mm installed in the electrode holder. Further information concerning the hardware and diagnostics are described elsewhere [11].

The experiments described here were done using a standard NSTX deuterium plasma with a current of  $I=0.8$  MA, a toroidal field of  $B=4.5$  kG, neutral beam heating power of  $P=2-4$  MW, and a lower-single-null diverted geometry with a discharge duration of  $\sim 0.5$  sec (#127046-054). These discharges had both H-mode and L-mode periods during biasing. The plasma density at the electrodes depended on the ‘outer gap’, i.e. the distance between the last closed flux surface and the outer midplane RF antenna limiter, which varied over the discharge from  $\sim 10$  cm to 5 cm for these experiments. Since these electrodes and probes were at least  $\sim 1$  cm behind the RF limiter, the measurements described in this paper were all made in the “far SOL” [12]. This electrode biasing did not cause any changes in the L-H transition time or the global plasma parameters, in contrast to biasing experiments in which the electrode was inserted farther into the plasma [13].

An example of electrode voltage and currents waveforms for one of these discharges is shown in Fig. 2. For this and all other cases described in this paper, electrode E2 was biased at -90 volts, electrode E3 was biased at +90 volts, electrode E4 was biased at -90 volts, and electrode #1 was floating (these three biased electrodes were all modulated in phase at 50 Hz). Thus the  $E_{\text{pol}} \times B$  drift direction between electrodes #2 and #3 (where the radial probe array was located) was in the outward radial direction. The biased electrode currents in the L-mode period were typically  $\sim 4$  amps in the positive electrode and  $\sim 0.5$  amps in the negative electrode during L-mode, and  $\sim 1/2$  this during H-mode. The (I,V) characteristic of these electrodes was nearly flat above about  $\pm 50$  volts, with a ratio of electron/ion saturation current of  $\sim 8$ . Also shown in Fig. 2 is the signal from probe P3b (between electrodes #2 and #3), which was biased steadily at +45 volts for this case, i.e. near electron saturation current. The electron density and temperature measured by this probe were  $n \sim 10^{11} \text{ cm}^{-3}$  and  $T_e \sim 8 \pm 5 \text{ eV}$  during biasing.

### 3. Effects of biasing on the SOL radial profiles

Figure 3 shows the effect of the electrode biasing of Fig. 2 on the radial profiles of the electron saturation current measured by the probes between

electrodes #2 and #3. The x-axis is the radial probe position with respect to the center of the electrodes, and each point represents the average over ~10-30 time periods of ~10 msec each for four discharges similar to Fig. 2, with either bias “on” or “off”. The electrode biasing causes an increase in all of the probe currents, e.g. by a factor of x2-5 for L-mode (0.3-0.4 sec) and x3-10 for H-mode (0.2-0.27 sec). These large changes were most likely due to an increase in electron density since the electron temperature did not change with biasing beyond the measurement error bars.

Fig. 4 shows the effect of this biasing on the floating potential profile during a similar shot. The bias caused a small (3-5 volt) increase in the floating potential for the two probes nearest the electrodes (P3a,P3b), but not for the probes farther out radially (P3c,P3d). In addition, no significant changes were seen in either the electron current or the floating potential in probe P2, which was between electrode #2 (-90 volts) and electrode #1 (floating). In general, a single negatively biased electrode had little or no effect on the local density or floating potential seen by probes on either side of it, while a single positively biased electrode caused an increase in the floating potential of both adjacent probes by about 5-20% of the positive electrode bias voltage.

## 5. Discussion

The main result of this experiment as shown in Fig. 3 was an increase in the plasma density between the biased electrodes by a factor of x3-10 with  $\pm 90$  volt biasing. This result is at least qualitatively consistent with the theory that the SOL density will increase when the local plasma is driven outward by the  $E_{pol} \times B$  drift created by biasing [1-3]. Thus a local control of plasma density in the far-SOL was demonstrated in this experiment. An additional result shown in Fig. 4 was that with biasing the floating potential increased by  $\sim 3-5$  volts between the electrodes, but not  $\sim 3$  cm radially behind the electrodes. Thus the biasing potential has a relatively short range across the magnetic field. Similar results have been seen in previous experiments on SOL biasing [8-10].

Some other results were obtained which can only be summarized here: (1) results similar to Fig. 3 were obtained in Ohmic and RF-heated plasmas with the same biasing configuration, i.e. this effect is similar in all types of plasmas in NSTX, (2) with the opposite polarity of biasing between electrodes #2 and #3, the density between these electrodes *decreased* significantly with respect to the no-biased case, i.e. showed the opposite behavior (as expected), (3) with electrodes #2 and #3 biased with respect to each other (i.e. ‘floating’), the effect on the SOL

density (and the current drawn by the electrodes) was significantly reduced, (4) the relative density fluctuations measured in the cases of Fig. 3 decreased by  $\sim x2$  with biasing, but the turbulence correlation lengths and times did not change significantly, (4) the effects of biasing were measured  $\sim 1$  m along B using the gas puff imaging diagnostic, but no significant effects on the density profile or SOL turbulence have yet been observed.

To compare the observed effects of biasing with theory, we would need to know how far the applied electric field penetrated along and across B. The applied (i.e. vacuum) field of  $\sim 180$  volts/cm *could* have created a  $v_{\text{rad}} \sim 5 \times 10^6$  cm/sec, i.e. up to  $\sim 50$  times more than the normal radial flow speed in this region. However, the effects on the SOL density are integrated along and across a field line, and so depend on the electric field penetration into the plasma, which in turn depends on the sheath physics [2,3] and cross-field mobility (e.g. viscosity, neutrals, turbulence) [14]. A discussion of these effects and the additional experimental results summarized above will be presented elsewhere.

Acknowledgments: We thank M. Bell, J. Boedo, R. Ellis, R. Maingi, and V. Soukhanovskii for help with the design and execution of these experiments. *This work supported by U.S. DOE Contract # DE-AC02-76CH03073.*

## References

- [1] Cohen, R.H. and Ryutov, D.D, Nucl. Fusion 37, 621 (1997)
- [2] Ryutov, D.D et al, Plasma Phys. Cont. Fusion 43, 1399 (2001)
- [3] Cohen, R.H. et al, Plasmas Phys. Cont. Fusion 49, 1 (2007)
- [4] D'Ippolito, D. A. et al, Phys. Fluids B **5**, 3603 (1993);  
Myra, J.R. et al Phys. Plasmas 3, 699 (1996)
- [5] Hara, J. et al, J. Nucl. Mat. 241-243, 338 (1997)
- [6] Counsell G. et al, J. Nucl. Mat. 313-316, 804 (2003);  
Counsell G. et al, 30<sup>th</sup> EPS Conference, Vol. 27A, P-3.202 (2003)
- [7] Stockel, J. et al, Plasma Phys. Cont. Fusion 47, 635 (2005)
- [8] Pitts, R.A. and Stangeby, P.C., Plasma Phys. Cont. Fusion 32, 1237 (1990)
- [9] Winslow, D.L. et al, Phys. Plasmas 5, 752 (1998)
- [10] Thomsen, H. et al, Plasma Phys. Cont. Fusion 47, 1401 (2005)
- [11] Roquemore, A.L. et al, to be published in RSI (Oct. 2008)
- [12] Ahn, J.-W., et al submitted to Phys. Plasmas (2008)
- [13] van Oost, G. et al, Plasma Phys. Cont. Fusion 54, 621 (2003)
- [14] Rozhanski, V.A., et al, Nucl. Fusion 39, 613 (1999);  
Carlson, A., Phys. Plasmas 8, 4732 (2001)

Figure Captions:

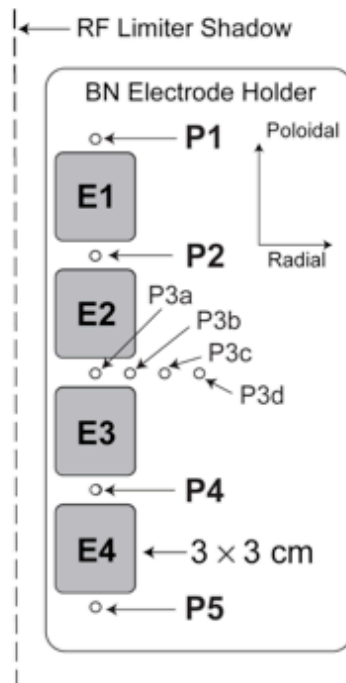
**Fig. 1:** Electrode and Langmuir probe configuration in this experiment. The four electrodes E1-E4 are 3x3 cm and flush-mounted into this boron nitride holding structure located just below the outer midplane of NSTX. The electrodes are separated in the poloidal direction and the local magnetic field was approximately normal to their surfaces. The 3 mm diameter probes P1-P5 are flush-mounted next to each electrode and also arrayed in the radial direction between electrodes #2 and #3 (P3a-P3d).

**Fig. 2:** Waveforms of typical electrode voltages and currents vs. time for the discharges described in this paper ( $B=4.5$  kG,  $I=0.8$  MA, #127054). Electrodes #2 and #3 were biased at -90 volts and +90 volts and drew currents of  $\sim 0.5$  Amps and  $\sim 4$  Amps (respectively). All electrode voltages were modulated at 50 Hz. At the bottom is the current from probe #P3b which was biased steadily at +45 volts in this discharge. The probe current increased each time the electrodes were biased, both before and after the H-L transition at 0.275 sec. For clarity, all of these waveforms were smoothed to reduce the large turbulent fluctuations.

**Fig. 3:** Effects of electrode bias on the radial profiles of probe electron saturation current as measured by probes P3a-P3d (#127046-054). The x-axis is the radial

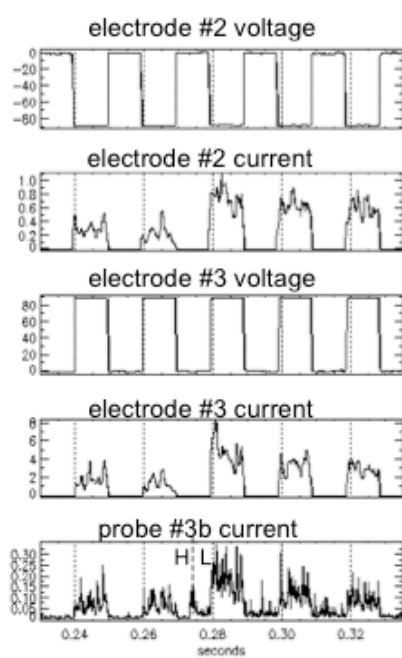
probe position with respect to the center of the electrodes. The probe currents all increase during biasing for both L-mode and H-mode conditions for this case in which the ExB drift was outward between electrodes E2 and E3.

**Fig. 4:** Effects of electrode bias on the radial profiles of floating potential as measured by probes P3a-P3d (#127052) for the same biasing as Fig. 3. The x-axis is the radial probe position with respect to the center of the electrodes. The floating potentials increased by 3-5 volts during biasing in the probes nearest the electrodes (P3a,b), but by much less in the probes farther outward (P3c,d).



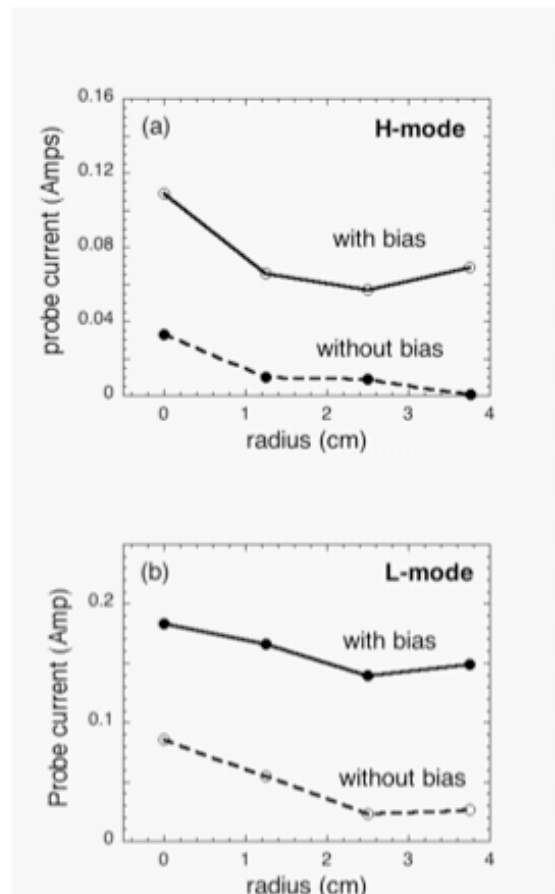
1

Fig. 1



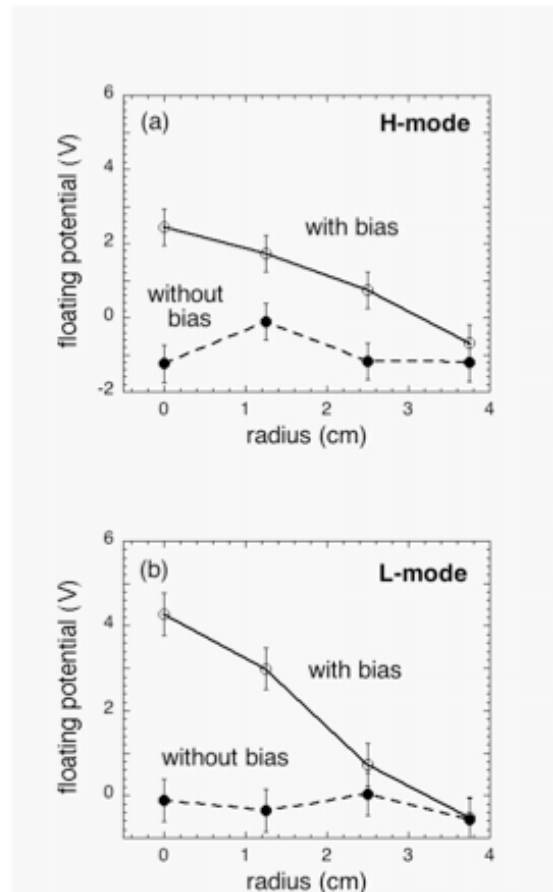
1

Fig. 2



1

Fig. 3



1

Fig. 4